

A Dynamical Model for the Globular Cluster G1

Holger Baumgardt¹, Junichiro Makino¹, Piet Hut², Steve McMillan³, Simon Portegies Zwart⁴

ABSTRACT

We present a comparison between the observational data on the kinematical structure of G1 in M31, obtained with the Hubble WFC2 and STIS instruments, and the results of dynamical simulations carried out using the special-purpose computer GRAPE-6. We have obtained good fits for models starting with single cluster King-model initial conditions and even better fits when starting our simulations with a dynamically constructed merger remnant of two star clusters. In the latter case, the results from our simulations are in excellent agreement with the observed profiles of luminosity, velocity dispersion, rotation, and ellipticity. We obtain a mass-to-light ratio of $M/L = 4.0 \pm 0.4$ and a total cluster mass of $M = (8 \pm 1) \times 10^6 M_\odot$. Given that our dynamical model can fit all available observational data very well, there seems to be no need to invoke the presence of an intermediate-mass black hole in the center of G1.

Subject headings: black hole physics—globular clusters: individual (G1)—methods: N-body simulations—stellar dynamics

1. Introduction

We report results from a series of N -body simulations for the globular cluster G1 in M31. G1 is one of the brightest and most massive globular clusters in the local group. Its total luminosity ($M_V = -10.94$ mag) and central velocity dispersion ($\sigma_0 = 25.1 \pm 1.7$ km/sec) are larger than those of any galactic globular cluster. (Meylan et al. 2001; Djorgovski et al. 1997),

¹Department of Astronomy, University of Tokyo, 7-3-1 Hongo, Bunkyo-ku, Tokyo 113-0033, Japan

²Institute for Advanced Study, Princeton, NJ 08540, USA

³Department of Physics, Drexel University, Philadelphia, PA 19104, USA

⁴Astronomical Institute “Anton Pannekoek”, Section computational science, University of Amsterdam, Kruislaan 403, 1098 SH Amsterdam, The Netherlands

Meylan et al. (2001) provided a standard multi-mass King model fit for G1. They found (for their model 4) a total mass of $15 \times 10^6 M_\odot$ and a core radius, half-mass radius, and tidal radius of 0.53, 13.2, and 187 pc, respectively. The estimated half-mass relaxation time was 50 Gyr, much longer than the Hubble time.

Gebhardt et al. (2002) have reported evidence for an intermediate-mass black hole of $2.0^{+1.4}_{-0.8} \times 10^4 M_\odot$ in the center of G1. Based on velocity profiles obtained with the Hubble space telescope’s STIS instrument, they constructed orbit-based axisymmetric models. Varying M/L and the mass of the central black hole, they found a best fit for $M/L = 2.5$ and $M_{BH} = 2 \times 10^4 M_\odot$. A model without a central black hole was rejected at a 2σ level.

The presence of such a black hole would be very interesting, for at least two reasons. First, it would lie neatly on the $M_{BH} - \sigma$ relation for galaxies (Tremaine et al. 2002; Merritt and Ferrarese 2001). Second, G1 would then be a perfect example of the type of cluster postulated by Ebisuzaki et al. (2001), some of which may find their way into the center of a galaxy by dynamical friction, where their intermediate-mass black holes may then merge to provide the seeds for supermassive black holes.

However, before embracing such an exciting conclusion it is all the more important to ensure that more conventional explanations of the observational data are ruled out. To this end, we have tried to construct the best possible evolutionary model for G1 as a large globular cluster that is still in an early phase toward core collapse, without harboring an intermediate-mass black hole. We have run a set of models with varying initial density profiles, half mass radii, total masses, and global M/L until we found a model that gave the best fit to the light and velocity profiles of G1.

In §2 we describe our numerical method. In §3 we present the results of simulations starting with a single non-rotating cluster, and in §4 we show what happens when we consider G1 to be the rotating product of two smaller globular clusters. We briefly summarize in §5.

2. Modeling Method

In order to model the evolution of G1 using N -body simulations, we face a scaling and a fitting problem: we can only handle $\sim 10^5$ particles while G1 contains $\sim 10^7$ stars; and we do not know which values to assign to the initial cluster model parameters such as the total mass and the half-mass radius. We solve the scaling problem by scaling the dynamical parameters in such a way as to reproduce in our model simulations the correct two-body relaxation time scales inferred for G1 from observations. We solve the fitting problem by

carrying out a large enough number of runs to allow us to isolate simulations that closely reproduce the observational data. Without the use of the GRAPE-6 computers (Makino et al. 2003) at Tokyo University, it would have been unpractical, if not impossible, to run the several dozen runs needed to determine our best fits, where each run consisted of a 64k-body simulation including stellar evolution and spanning a Hubble time.

We used Aarseth’s N -body code NBODY4 (Aarseth 1999). All simulated clusters contained $N = 65,536$ stars initially, with a range of masses following Kroupa (2001)’s mass function with lower and upper mass limits of 0.1 and $30 M_{\odot}$, respectively. Our simulations did not contain primordial binaries, which is a reasonable simplification for a cluster that is still quite far from core collapse. We did not include M31’s galactic tidal field, which would have a negligible influence at the position of G1, at least 40 kpc from the center of M31. Since tidal effects are unimportant, we are left with two evolution mechanisms: stellar evolution and two-body relaxation.

Stellar evolution was modeled according to the fitting formulae of Hurley et al. (2000), which give stellar lifetimes, luminosities and radii as functions of initial stellar mass and metallicity for all stages of stellar evolution. For our runs we took a metallicity of $[\text{Fe}/\text{H}] = -0.95$, similar to the mean metallicity of G1 as determined by Meylan et al. (2001). We assumed a retention fraction of neutron stars of 15%.

We assumed an age of 12 Gyr for G1. All simulations were carried out for 13 Gyr and the final density and velocity profiles were obtained from 10 snapshots spanning a 500 Myr period centered at $T = 12$ Gyr. For the comparison of our models with the observations of G1, we assume a distance of 770 kpc to M31, so one arcsecond corresponds to 3.7 pc. Typically, about 1% of the stars escaped from the cluster during a simulation. For comparisons with observations, we used only stars which were still bound to the cluster at $T = 12$ Gyr.

Since N -body calculations cannot yet handle millions of particles, we have to scale the parameters of our simulations in order to match the most important stellar evolution and stellar dynamical parameters of the actual G1 cluster. In order to match the relaxation time of G1, we have to increase the radius of our cluster. The relaxation time of a cluster with mass M and half-mass radius r_h is given by Spitzer (1987) as

$$T_{rh} = 0.138 \frac{\sqrt{M} r_h^{3/2}}{\langle m \rangle \sqrt{G} \ln(\gamma N)} , \quad (1)$$

where $\langle m \rangle$ is the mean mass of the stars in the cluster, N the number of stars, and γ is a factor in the Coulomb logarithm, approximately equal to 0.02 for multi-mass clusters (Giersz and Heggie 1996). In order to reproduce the same value of T_{rh} , the half-mass radius

must therefore be equal to

$$r_{hS} = r_{hG1} \cdot \left(\frac{N_{G1}}{N_S} \right)^{1/3} \left(\frac{\ln(\gamma N_S)}{\ln(\gamma N_{G1})} \right)^{2/3}, \quad (2)$$

where subscripts $G1$ and S denote, respectively, the actual values for $G1$ and those used in our simulations.

In the first set of simulations, we started from King model initial conditions, with dimensionless central concentrations in the range $4.0 \leq W_o \leq 11.0$. For each choice of initial density profile, we ran full simulations for a number of choices for the initial physical half-mass radius $r_h(t = 0)$ and mass $M(t = 0)$ of $G1$ until we could fit the surface density profile of Meylan et al. (2001) over a maximum range in radius while simultaneously obtaining an optimal fit to the observed velocity profile. For the surface density, we scaled our predicted profile by a multiplicative factor to obtain the best fit (in practice changing the M/L predicted by our assumed IMF by a factor of $1.5 \sim 2$). For the velocity profile, we used the symmetrized profile shown by Gebhardt et al. (2002) in their Fig. 1 and the ground-based value of Djorgovski et al. (1997), who measured a velocity of 25.1 ± 1.7 km/sec inside an aperture of $1''.15 \times 7''.0$. For each run, a best fit was determined by a χ^2 test against the combined data. With improved estimates for $r_h(t = 0)$ and $M(t = 0)$, a new initial half-mass radius could be calculated and a new simulation was performed. Simulations were performed until the half-mass radius changed by less than 5% between successive iterations. A more detailed description of our simulations and their results will be presented in a forthcoming paper (Baumgardt et al. 2003).

3. Single Cluster Simulations

Figure 1 shows the data for the best fit from among the runs where we started with a single cluster in the form of a King model; here the initial central potential depth was $W_o = 7.5$. The top panel shows the inferred projected luminosity density. We can see that the fit is very good for $r < 15$ pc. The reason why the model density drops off sharply at large radius is because the initial King model had a tidal radius of 32 pc if we scale it to $G1$. Two-body relaxation begins to produce an extended halo with a surface density slope ~ -4 , but a Hubble time is too short to let this effect propagate very far into the observed halo. Starting from deeper King models ($W_o = 8$ or higher) does not solve this problem: such models predict too high a surface density around $r = 10$ pc, while still falling short at larger radii. The implication is that $G1$ must have started with a density distribution more extended than any King model that can be fit to the bulk of the stars.

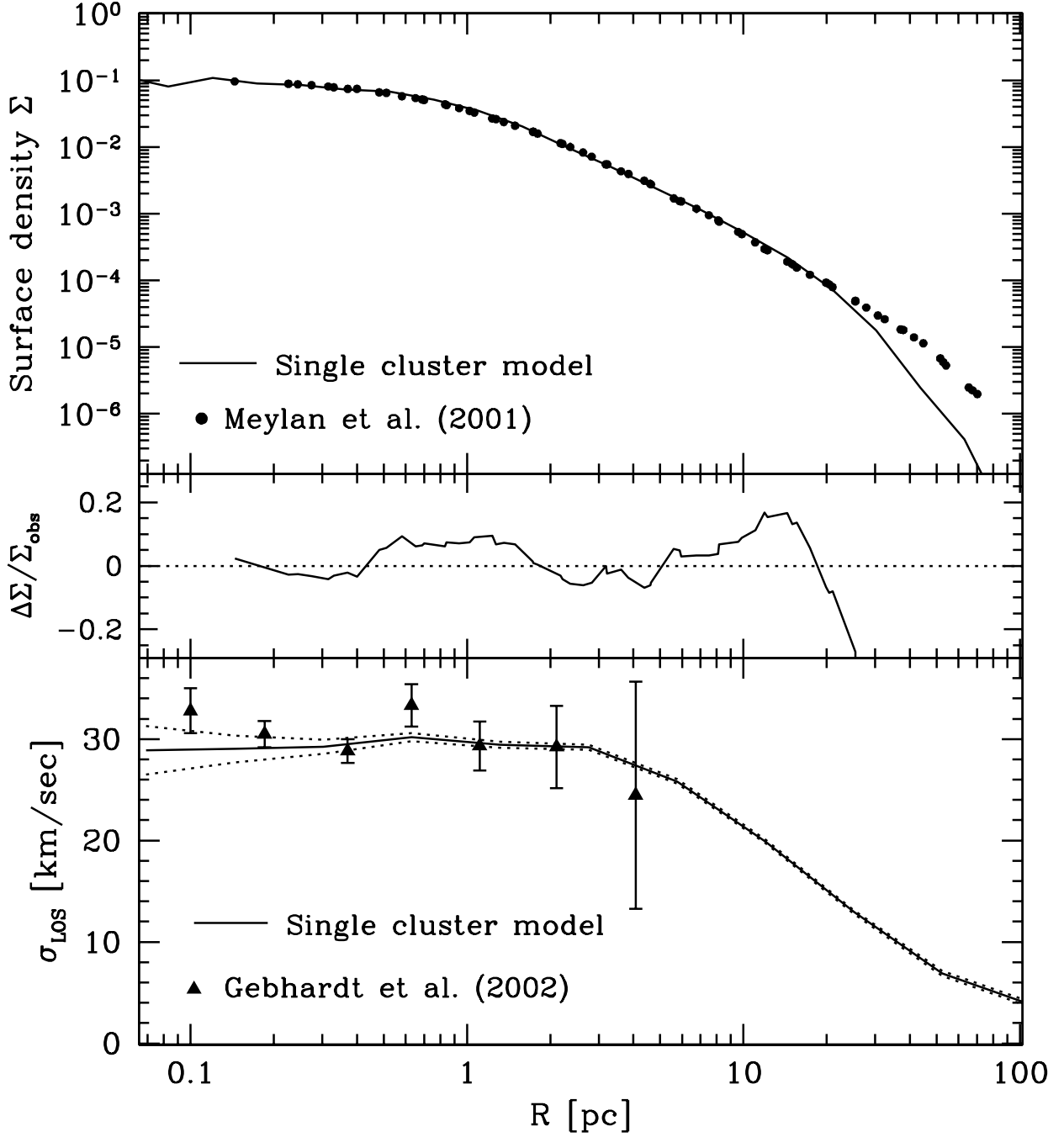


Fig. 1.— The best-fit result, starting from a single $W_o = 7.5$ King model. The top panel shows the surface luminosity profile Σ of the simulations (full line) and the observations (filled circles). The middle panel shows $\Delta\Sigma/\Sigma_{\text{obs}}$, where $\Delta\Sigma = \Sigma_{\text{model}} - \Sigma_{\text{obs}}$. The bottom panel shows the velocity dispersion in the simulations (solid curve, with dashed curves indicating the 1σ error) and observations (filled triangles with error bars).

The bottom panel shows the velocity dispersion inferred from our $W_o = 7.5$ model, as compared to the dispersion observed by Gebhardt et al. (2002). For larger W_o values, our models produce velocities that are too high at the largest observed radii. Models with slightly lower concentration gave a somewhat better fit, but when we require the model to reproduce the density as well, the combined requirements clearly point to $W_o = 7.5$ as producing the best agreement, and one which falls within the observational errors everywhere except near the tidal radius artificially imposed by the initial conditions; we address this limitation in the next section.

Note that our model cluster has a central potential much shallower than the multi-mass King model fit by Meylan et al. (2001); indeed, our total mass is only about half of what they derived. Their extreme values stem from the implicit King-model requirement that a model should be completely (two-body) relaxed, which is unphysical in the outer regions where the relaxation time is much longer than a Hubble time. Since these outer regions cannot yet be relaxed, mass segregation has not been able to deliver massive stars from there to the central regions. Using a King model to fit the current state of the cluster forces *all* massive stars to condense toward the center, hence leading to values for W_o and total mass that are far too high.

To sum up, an evolutionary model starting from a King model without initial mass segregation reproduces both the luminosity profile and the velocity dispersion profile of G1 rather well. The fits are not perfect, though, on two counts. First, the best-fit model still produces too steep a luminosity profile at larger radii. Second, since we start from a spherically symmetric non-rotating model, in principle we cannot fit the observed rotation profile or ellipticity. The question is whether we can introduce rotation while simultaneously at least preserving, and hopefully improving, the reasonable fits obtained so far. In the next section we answer this question affirmatively.

4. Merger Simulations

Currently favored scenarios for the formation of star clusters are the collapse of giant molecular clouds or the collision of smaller clouds (Fall and Rees 1985; Fujimoto and Kumai 1997). A collision scenario could easily explain the apparent rotation of G1. It might also account for the run of surface density in the halo, since simulations of the merging of two stellar systems usually give surface density profiles $\Sigma(R) \sim R^{-3.0}$ (Sugimoto and Makino 1989; Makino, Akiyama, & Sugimoto 1990; Okumura et al. 1991). In addition, Theis (2002) recently described a formation scenario in which star clusters form from collapsing shells of gas and found that over a large range of galactocentric radii these shells are likely to evolve

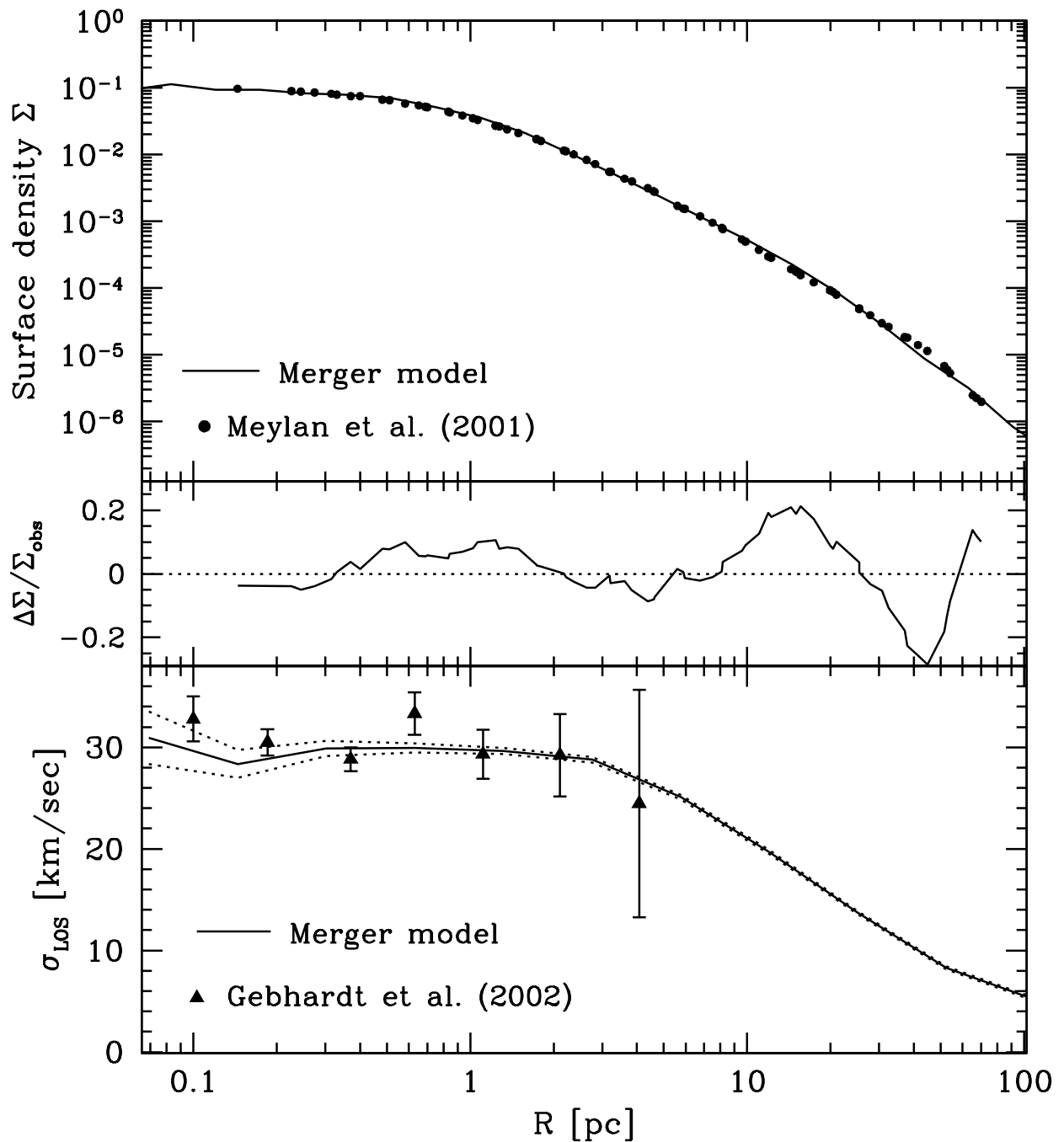


Fig. 2.— Same as figure 1, but for the merger model that started from two $W_o = 6.5$ King models.

into twin clusters, about 1/3 of which later merge to form single stellar systems.

Based on these theoretical hints, we have carried out a series of simulations starting with an early merger of two star clusters. For the sake of simplicity, we have restricted ourselves to the merger of two identical King model clusters on parabolic orbits with initial separation $r_i = 20$ and pericenter separation in N -body units (Heggie & Mathieu 1986) of $p = 1$ (another simulation with $p = 2$ gave similar results). We used $N = 80,000$ stars in our merger simulation without including stellar evolution, a reasonable approximation given that our merger was postulated to occur during formation of the clusters. Since no significant relaxation effects can occur in such a short time, for simplicity we used only equal-mass stars. After the merger product had undergone its violent relaxation, we randomly selected 65,536 stars from among all the stars still bound to the final cluster remnant, and assigned masses drawn from a Kroupa (2001) IMF to them. With this recipe for the initial conditions, we then started our dynamical evolution simulations, for a duration of $T = 13$ Gyr.

Fig. 2 shows the final density and velocity dispersion profiles for our best-fit simulations which started with a collision between two $W_o = 6.5$ initial King models. Note that our simulations now reproduce the observed extended halo very well. The agreement between the observed and model velocity dispersions is also very good.

Figure 3 compares the rotation and ellipticity profiles of our merger model and the observations. We measured the rotation profile from two directions perpendicular to each other and the minor axis and took the mean of the two directions. The profiles were determined from the radial velocities of all bright stars located in an area between angles of 10° and 40° with respect to the major axis, in order to make an optimal comparison with Gebhardt et al. (2002), who performed their HST/STIS spectroscopy at an angle of 25° against the major axis. The agreement between simulated and observed rotation profiles is very good.

Similarly, the ellipticity profile of our merger run is in good agreement with the ellipticity profile of G1 as determined by Meylan et al. (2001), (as can be seen in the lower panel of Fig. 3). The N -body run starts with a near constant ellipticity of about $\epsilon = 0.25$. After $T = 12$ Gyr, the cluster core has become almost spherical due to relaxation effects, while the halo ellipticity has remained unchanged. The observations show a similar drop of ϵ towards the core. The fact that our data do not seem to give a good fit in the innermost region is not significant: the observational evidence for an ellipticity of $\sim 10\%$ within the inner parsec relies on measuring a flattening of $\lesssim 0.1\text{pc}$, corresponding to $\lesssim 0.03''$, smaller than the resolution of HST's PC on WFPC2.

Table 1 summarizes our results for the best-fitting models. It shows W_o for each initial model, as well as the half-mass radius r_h at $T = 12$ Gyr, and the inferred total mass M and

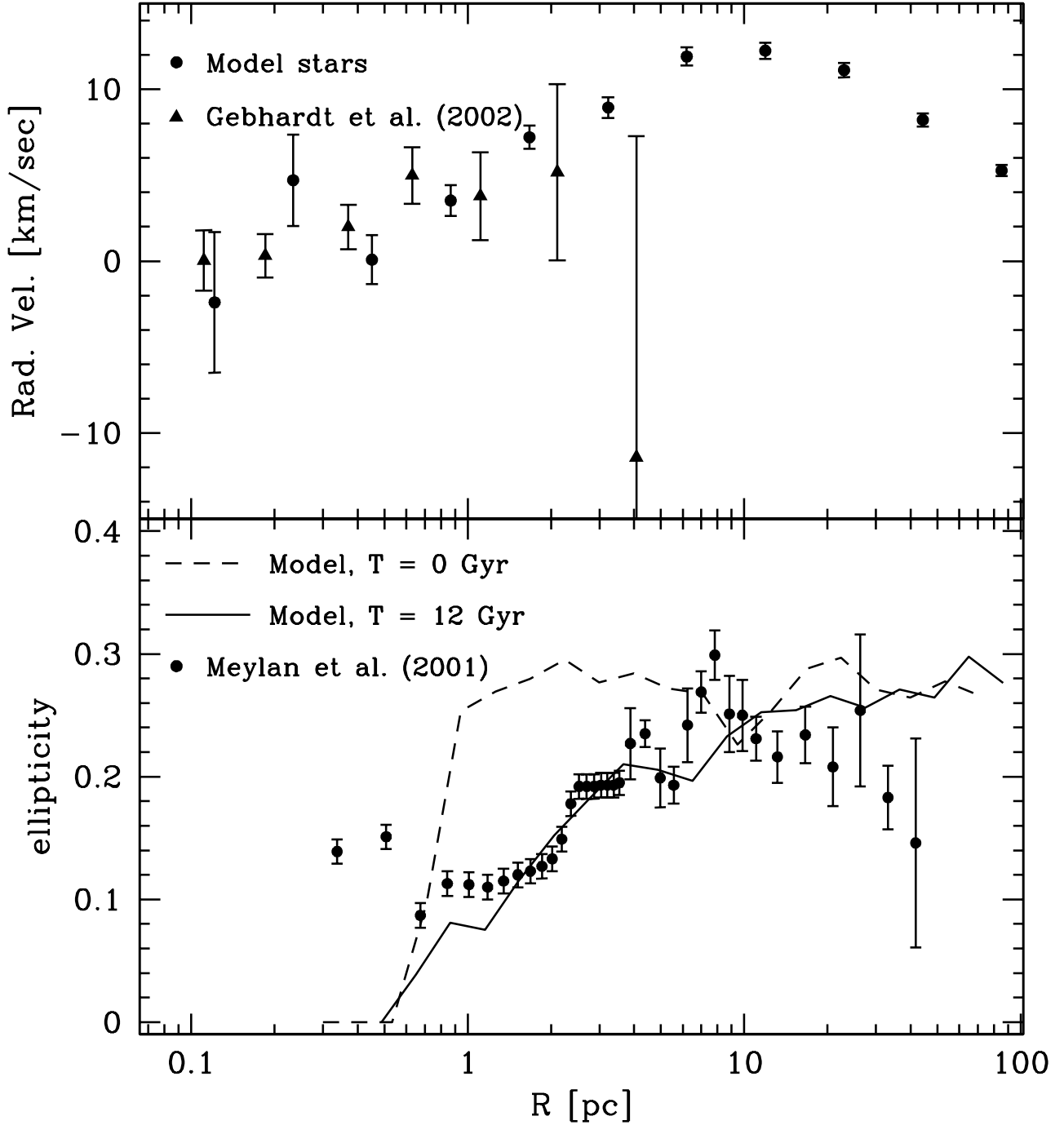


Fig. 3.— Symmetrized radial velocities (top panel) and ellipticity profiles (bottom panel) for the observations and our best-fit merger model. The ellipticity is defined as $\epsilon = 1 - b/a$, where a and b are the major and minor axis of the best-fit ellipse for the observations and the projected model data. In the bottom panel, the dashed line corresponds to the initial conditions for the simulation, just after the merger, while the full line corresponds to the model after 12 Gyrs.

Table 1: Results of the best-fitting N -body runs.

W_0	Type	r_h [pc]	M [M_\odot]	M/L	P_V
7.5	Single	8.47	$(7.60 \pm 0.76) \times 10^6$	3.80 ± 0.38	0.20
6.5	Merger	8.13	$(8.20 \pm 0.85) \times 10^6$	4.10 ± 0.42	0.28

M/L required to give the best-fit velocity dispersions. The errors given for both quantities are the statistical errors from the χ^2 -fit. The last column gives the probability P_V that our velocity distribution agrees with the observations of Gebhardt et al. (2002) and Djorgovski et al. (1997), determined from a χ^2 -test against the combined data.

The mass-to-light ratios we obtain in our best fits lie around $M/L \sim 4$, relatively large but still within the range of mass-to-light ratios observed for galactic globular clusters (Pryor and Meylan 1993). Our success in modeling G1 as a merger product does not necessarily imply that a merger history is the only way to explain its current state. For example, it is also possible that G1 is a heavily stripped remnant of a dwarf spheroidal. What is important is that the observed rotation can be well modeled under at least one set of reasonable assumptions, as we have shown here. The presence of rotation does not invalidate attempts at modeling under the simpler assumption of spherical symmetry; rather it invites a further fine-tuning of the already good agreement of spherical models.

5. Conclusions

We have constructed evolutionary models for the massive globular cluster G1. Starting from a $W_o = 7.5$ King model we can reproduce both the observed luminosity profile for $r < 15$ pc and the observed velocity dispersion profile. A model starting from the merger of two $W_o = 6.5$ King models fares even better: it can reproduce the luminosity, velocity dispersion, rotation profiles and ellipticity for the entire range of observations.

Our simulations were motivated by the recent claim of evidence for a massive central black hole. Given that our dynamical model without central black hole can fit all available observational data very well, there seems to be no need to invoke the presence of an intermediate-mass black hole. Note that we obtained an excellent fit by varying only the following basic parameters: the central potential W_o , the initial total mass $M(0)$ and total mass-to-light ratio M/L , and the initial half-mass radius $r_h(0)$. Our conclusions are therefore robust, and independent of any fine tuning in initial conditions.

This work is the first example of the successful detailed dynamical modeling of the evolution of a globular cluster with rotation. We have shown how N -body simulations have reached maturation as the most powerful tool to interpret detailed observational data, obviating the need for simplifying assumptions such as spherical symmetry or the use of static (*e.g.* multi-mass King) models.

Acknowledgments

The authors thank Toshi Fukushige and Yoko Funato for stimulating discussions and Karl Gebhardt for sharing his velocity data on G1 with us. We are especially grateful to Sverre Aarseth for making the NBODY4 code available to us and his constant, untiring help with the code. This work is supported in part by Grant-in-Aid for Scientific Research B (13440058) of the Ministry of Education, Culture, Science and Technology, Japan, by NASA ATP grant NAG5-10775 and by the Royal Dutch Academy of Science (KNAW) and Dutch organization for Scientific Research (NWO).

REFERENCES

Aarseth, S. J. 1999, PASP, 111, 1333

Baumgardt, H., Makino, J., Hut, P., McMillan, S.L.W., and Portegies Zwart, S.F. 2003, in preparation

Djorgovski, S. G., Gal, R. R., McCarthy, J. K., Cohen, J. G., de Carvalho, R. R., Meylan, G., Bendinelli, O., and Parmeggiani, G. 1997, ApJ, 474, L19

Ebisuzaki, T., Makino, J., Tsuru, T.G., Funato, Y., Portegies Zwart, S.F., Hut, P., McMillan, S.L.W., Matsushita, S., Matsumoto, H., and Kawabe, R. 2001, ApJ, 562, L19

Fall, S. M., and Rees, M. J. 1985, ApJ, 298, 18

Fujimoto, M., and Kumai, Y. 1997, AJ, 113, 249

Gebhardt, K., Rich, R. M., and Ho, L. C. 2002, ApJ, 578, L41

Giersz M., Heggie D. C. 1996, MNRAS, 279, 1037

Heggie, D. C. & Mathieu, R. D. 1986, LNP Vol. 267: The Use of Supercomputers in Stellar Dynamics, 233

Hurley, J. R., Pols, O. R., and Tout, C. A. 2000, MNRAS, 315, 543

Kroupa, P. 2001, MNRAS, 322, 231

Makino, J., Akiyama, K., & Sugimoto, D. 1990, PASJ, 42, 205

Makino, J., Fukushige, T., and Namura, K. 2003, in preparation

Merritt, D., and Ferrarese, L. 2001, ApJ, 547, 140

Meylan, G., Sarajedini, A., Jablonka, P., Djorgovski, S. G., Bridges, T., and Rich, R. M. 2001, AJ, 123, 830

Okumura, S. K., Ebisuzaki, T., and Makino, J. 1991, PASJ, 43, 781

Pryor C., and Meylan, G. 1993, in *Structure and Dynamics of Globular Clusters*, eds. S. Djorgovski, G. Meylan, ASP Conference Series 50, p. 357

Spitzer, L. J. 1987, *Dynamical Evolution of Globular Clusters*. Princeton University Press, Princeton, New Jersey.

Sugimoto, D., and Makino, J. 1989, PASJ, 41, 1117

Theis, C. 2002, Ap&SS, 281, 97

Tremaine, S., Gebhardt, K., Bender, R., Bower, G., Dressler, A., Faber, S. M., Filippenko, A.V., Green, R., Grillmair, C., Ho, L.C., Kormendy, J., Lauer, T.R., Magorrian, J., Pinkney, J., and Richstone, D. ApJ, 574, 740